e-PS, 2013, **10**, 1-9
ISSN: 1581-9280 web edition
ISSN: 1854-3928 print edition

e-Preservation Science (e-PS)

is published by Morana RTD d.o.o.
www.Morana-rtd.com

SCIENTIFIC PAPER

This paper is based on a presentation at the 10th International Conference of the Infrared and Raman Users Group (IRUG) in Barcelona, Spain, 28-31 March 2012.

Guest editors:
Prof. Dr. Jose Francisco Garcia Martinez and Dr Anna Vila

1. Getty Conservation Institute, 1200 Getty Center Drive, Suite 700, Los Angeles, CA 90049, USA

2. Winterthur Museum, Conservation Department, 5105 Kennett Pike, Winterthur, DE 19735, USA

3. Department of Physics, University of Wisconsin-Milwaukee, 1900 East Kenwood Blvd., Milwaukee, WI, USA

corresponding author:
cpatterson@getty.edu

received: 02/06/2012
accepted: 14/01/2013

key words:
FTIR imaging, cross-section, synchrotron radiation, IRENI, IRUG 2012

Synchrotron-based Imaging FTIR Spectroscopy in the Evaluation of Painting Cross-sections

Catherine Schmidt Patterson[1]*, David Carson[1], Alan Phenix[1], Herant Khanjian[1], Karen Trentelman[1], Jennifer Mass[2], Carol Hirschmugl[3]

Abstract

A recently commissioned mid-infrared synchrotron beamline (IRENI) at the Synchrotron Radiation Center (SRC) in Stoughton, WI, provides wide-field illumination for an FTIR microscope equipped with a focal plane array (FPA) detector by bundling and collimating 12 beams extracted from the synchrotron source. This unique design enables Fourier transform infrared (FTIR) imaging applications that require the brightness of a synchrotron and allows the collection of high signal-to-noise FTIR hyperspectral data cubes, providing images with high diffraction-limited resolution in a relatively short time frame. A selected group of prepared cross-section samples – mockups containing thin layers of organic material and layers of materials containing similar chemical moieties, and a sample from a real work of art – were analyzed in order to evaluate the utility of the IRENI beamline for the examination of samples relevant to cultural heritage. The results suggest that the high resolution imaging obtainable by IRENI is ideally suited to address some of the challenges related to the analysis of the small multi-layered inorganic/organic composite samples commonly found in cultural heritage research.

1 Introduction

Organic components in works of art or other objects of cultural heritage significance can include a diverse range of materials including canvas or other textiles, cellulose, organic colorants, resins, varnishes, and binding media such as glues, waxes, oils, gums, or egg. These materials may be found singly or mixed with other organic or inorganic materials, and are often components in objects with a complex stratigraphy, e.g. a painting or painted sculpture. Analysis of organic compounds in cultural heritage materials has long relied on the use of optical microscopy (including cross-section photomicroscopy using ultraviolet and visible illumination),[1,2] gas chromatography- and liquid chromatography-mass spectrometry (GC-MS and LC-MS),[2-8] and, importantly, infrared spectroscopy.[2,9-16]

Fourier transform infrared (FTIR) microscopy of samples from works of art can provide specific identification of organic – as well as some inorganic – compounds,[9] but can be challenging since the organic materials often are present as part of complex mixtures or as thin layers on the order of a few microns thick, below the spatial resolution limits of many instruments. The continued development of attenuated total reflection (ATR)-FTIR,[15,17,18] FTIR mapping and imaging techniques,[17,19-25] and synchrotron-based FTIR[18,21,23,26-34] are beginning to address these challenges. Indeed, new synchrotron facilities around the world with cultural heritage research as a component of their user groups continue to be introduced.[31,34,35]

This paper presents recent work evaluating a new mid-infrared imaging synchrotron beamline (called IRENI–infrared environmental imaging) at the

Synchrotron Radiation Center (SRC) in Stoughton, WI, for the analysis of cultural heritage materials. The IRENI beamline is unique in the field of synchrotron-based FTIR imaging because it enables wide-field, high resolution infrared imaging with the high throughput and signal-to-noise produced by a bright, stable synchrotron beam.[36] The high resolution imaging obtained with IRENI is diffraction-limited across the mid-IR[36,37] (~800-3950 cm^{-1}) and builds on the successful application of synchrotron radiation-FTIR in cultural heritage research[18,21,23,26-30,32-34] by providing new capabilities that address some of the challenges related to the analysis of small, multi-layered cross-section samples.

To assess the potential of the IRENI system for the analysis of cultural heritage samples, experiments were performed on prepared cross-section samples representative of the types of layering and organic materials typically found in paintings. The data collected demonstrate that the IRENI system is capable of (I) simultaneous detection and imaging of multiple layers in complex matrices; and (II) identifying both organic and inorganic materials with high spatial resolution. Such promising early results suggest that chemical imaging through FTIR analysis at the IRENI beamline may provide an important analysis tool for the challenging layered microstructures frequently encountered in samples from works of art and other objects of cultural heritage significance.

2 Materials and Methods

Details of the IRENI beamline have been published elsewhere.[25,36,37] Briefly, the beamline uses a large swath of infrared radiation from the synchrotron, and separates that radiation into a bundle of 12 collimated beams to illuminate up to a 60×40 μm^2 area of the sample plane of a commercial IR microscope (Bruker Vertex 70 FTIR/Hyperion 3000 microscope) equipped with a 128×128 pixel HgCdTe focal plane array detector (FPA, Santa Barbara Focalplane). In transmission mode, a condenser is used to slightly defocus the collimated beams to homogenously illuminate as much of the detector area as possible. Because the optics, optical path, and pixels at the detector define the geometric area at the sample plane that is detected by each pixel, no apertures are needed to define the sampling area. The effective pixel size is determined by the magnification of the effective geometrical area at the sample plane by the microscope objective. In the imaging setup at the IRENI beamline, the highest spatial resolution is achieved by choosing an effective pixel size at the detector that spatially oversamples the data. Several combinations of objectives/condensers are available for use at the beamline; as typically configured for transmission measurements (with a 74×/0.6 N.A. Schwarzschild objective (Ealing) and 15×/0.58 N.A. Schwarzschild condenser (NicPlan)), the effective geometrical pixel area at the sample plane is 0.54×0.54 μm^2, equivalent to that achieved in ATR-FTIR. However, because the IRENI setup operates in transmission, there is no contact between the sample and an objective, as is required with ATR. The IRENI experimental setup achieves diffraction-limited chemical imaging in less time than is achievable by other FTIR beamline systems. Data was collected using the commercial OPUS software suite (Bruker) and analyzed using a program generated in-house at SRC called IRidys, which runs in the commercial software package IGOR Pro and is made freely available to researchers.[38]

The IRENI beamline may be able to address the existing challenges in FTIR analysis as applied in cultural heritage research, namely the presence of materials in complex mixtures or layers sufficiently thin to be below the spatial resolution limits of many instruments, and the spatial discrimination of chemical related species. Thus, three types of samples were studied to assess the ability of the IRENI system to: (i) achieve spatially resolved identification of thin layers of organic material; (II) simultaneously detect chemically similar layers; and (III) produce meaningful results from samples from real works of art. Materials used include oxygen barrier film FR-7750 (Bell Fibre Products), which was used as acquired. Rabbit skin glue (Utrecht) prepared in-house, and egg yolk from a commercial egg were used to create a painting mock-up containing two chemically similar organic materials. A layer of prepared rabbit skin glue was painted onto a prepared wooden panel coated with gypsum ($CaSO_4 \cdot 2H_2O$), which had been dried and sanded to form a smooth surface. Once the glue layer was dry, a layer of egg yolk was added in several coats. Several samples from the early twentieth century (1905-1906) painting *Le Bonheur de vivre*, also called *The Joy of Life,* by Henri Matisse (The Barnes Foundation, BF719, Philadelphia, PA) were also provided for analysis.

Samples to be prepared as cross-sections were removed by hand using a scalpel with either a 1 mm or size 11 steel blade (or cut from the bulk with scissors in the case of the film sample), mounted in Bio-Plastic® Liquid Casting Plastic (Ward's Natural Science), and cured using ~½ the recommended volume of catalyst. The resulting semi-hard resin block was cut to expose the stratigraphy of the sample using an ultramicrotome (PowerTome XL, RMC Products) fitted with a diamond knife (Ultra 45°, DiATOME). Transmission experiments require a thin section (typically <~5 μm, but occasionally up to ~10 μm thick) of the cross-section.[30,33] For transmission experiments on the IRENI beamline, microtome slices containing the full stratigraphy, each ~3 μm thick, were cut from the block face and retained. Through trial and error, 3 μm was found to be the smallest thickness to which most samples (of varying friability) could be reproducibly cut before damage in the form of sample loss began to occur.

This sample preparation method was selected to be compatible with other analytical techniques utilized in cultural heritage science: the block face containing the fully exposed stratigraphy of the sample is available for analysis by optical microscopy (visible and ultraviolet illumination), elemental analysis using scanning electron microscopy-energy dispersive X-ray spectroscopy (SEM-EDS), and compositional analysis using Raman or FTIR microspectroscopy. The block face samples were also examined at IRENI in reflection mode but results from these tests are beyond the scope of this paper. Samples, both block face and transmission samples, were retained following analysis at the Getty Conservation Institute for future use.

3 Results and Discussion

3.1 Analysis of Model Layered Samples

A cross-section of a sample of the FR-7750 oxygen barrier film was analyzed to assess the capabilities of the IRENI system for discriminating closely spaced layers of organic material. The film contains four clearly delineated layers (Figure 1a) – three 10-20 μm thick layers of chlorotrifluoroethylene (CTFE), low density polyethylene (LDPE), and polyester, and a ~65 μm thick layer of LDPE[39] – thus providing a good model for the layered systems that are commonly found in painting cross-sections. The polyester mounting resin in which the film is mounted provides an additional chemical signature identifiable by FTIR.

Initial experiments on this layered sample were performed to compare the spectral quality provided by the synchrotron source to that provided by the Vertex 70 thermal source at the IRENI end station at a given pixel resolution and experimental parameter set. FTIR images were collected from the thin section sample (supported on a BaF_2 window), using a 74× objective and 15× condenser. A ~35×35 μm^2 area was illuminated in this configuration (64×64 pixels, each pixel with an effective area at the sample plane of 0.54×0.54 μm^2). This configuration thus collects a total of 4,096 individual FTIR spectra, each the sum of 128 scans, simultaneously in <5 min. Each image map was acquired by collecting a mosaic of 6 tiles of this size (covering a total area of ~35×207 μm^2 in ~30 min, and containing 24,576 individual spectra). From the resulting data cubes, spectra were extracted from individual pixels to compare spectral quality between the thermal and synchrotron sources. Results from the thermal and synchrotron sources are shown in Figures 1b and 1c, respectively.

While the three different materials found in the film and the polyester embedding resin are clearly identifiable in the spectra acquired using the thermal source (Figure 1b), the baselines are noisy and the weakest features in each spectrum become difficult to distinguish, particularly in the spectrally congested regions of the two polyesters between 1200-1700 cm^{-1}. The spectra acquired using the synchrotron source (Figure 1c) clearly demonstrate the expected signal-to-noise ratio improvement: weak features at 1506, 1577, and 1616 cm^{-1} become discernable in the film's polyester

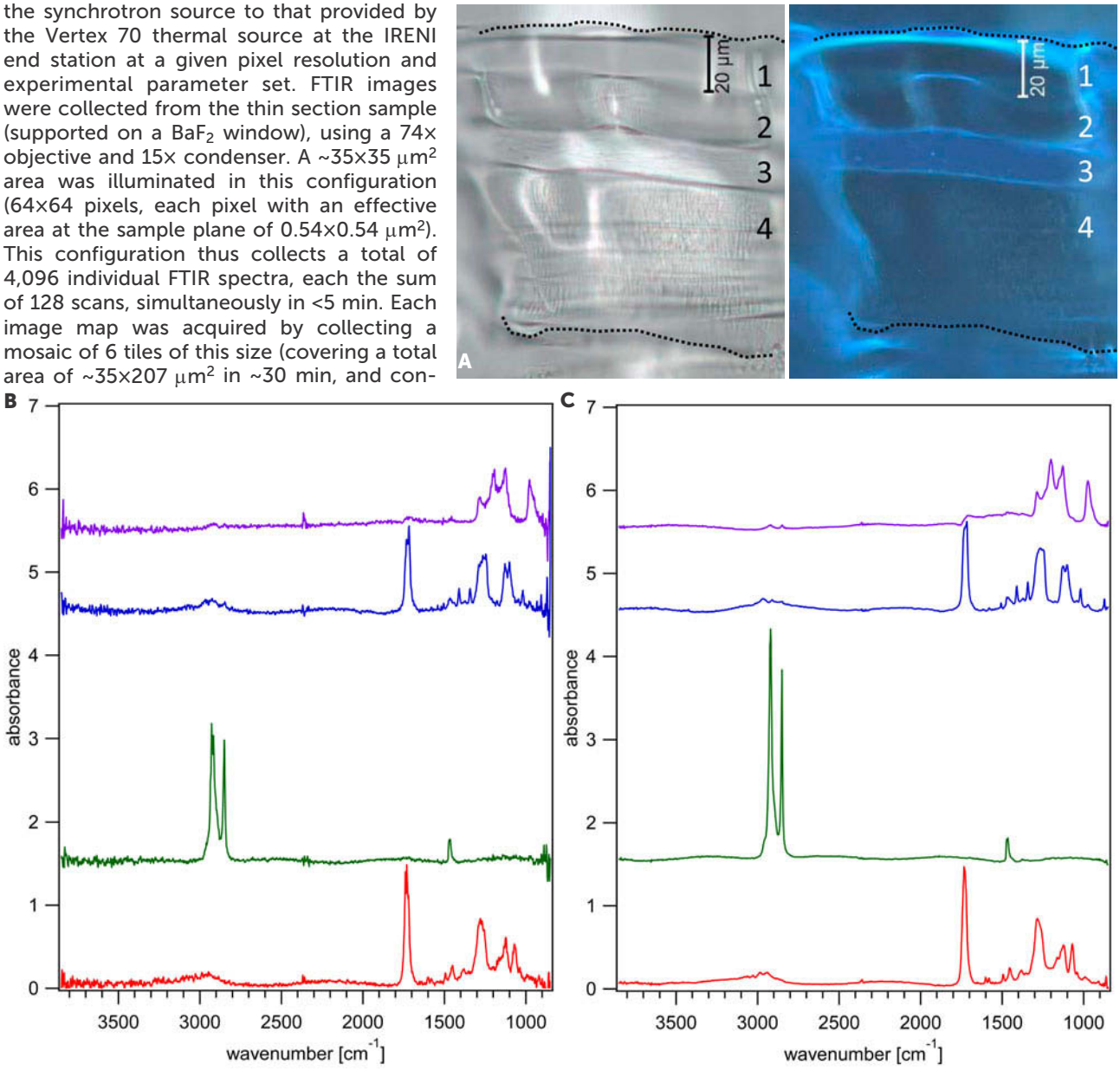

Figure 1: (A) Photomicrographs of the oxygen barrier film cross-section (with CTFE, LDPE, polyester, and LDPE layers labeled 1-4, respectively), photographed under white light (left), and ultraviolet illumination (right); dashed lines indicate top and bottom edges of the embedded cross-section. Single pixel spectra from chemical images obtained using (B) a thermal source and (C) the synchrotron light source. In (B) and (C), the four spectra shown are (from bottom to top) the polyester embedding resin, LDPE (layer 4), polyester (layer 3), and CTFE (layer 1) layers of the film. The spectra shown come from the same pixel locations for the two sources. All spectra are averages of 128 scans, and are offset for clarity.

layer, for example. The ability to distinguish minor features such as these increases the overall likelihood of being able to differentiate chemically related materials, whose most intense IR absorbances are expected to be quite similar. In this sample, for example, both polyesters exhibit an intense band between ~1225-1320 cm^{-1}, and the carbonyl band is located between ~1675-1770 cm^{-1} for each. These normally diagnostic features therefore cannot be used to distinguish the two materials. Less intense bands, more clearly identifiable and baseline resolved when using synchrotron radiation than in the comparable thermal spectra, must be utilized instead.

Since the synchrotron source provides increased sensitivity with respect to thermal sources, even if fewer scans are averaged the resulting spectra are sufficiently detailed to allow efficient chemical imaging in a short space of time. Figure 2 shows results from a data set collected from a larger area of the same cross-section sample of the oxygen barrier film, but averaging only 32 scans per pixel (compared to 128 scans per pixel shown in Figure 1b). In this analysis, 15 tiles (covering a total area of ~104x173 μm^2 and containing 61,440 individual spectra) were collected in ~20 min; a photomicrograph of the analyzed area taken under white light illumination is shown in Figure 2a. Figure 2b shows a series of individual pixel spectra extracted from a single line across the sample, along the path noted on Figure 2a. The variation of the spectra along this line corresponds well with the suspected positions and relative thickness of the layers. Despite averaging fewer scans, the single pixel spectra obtained using the synchrotron source are sufficiently detailed to allow identification of spectral features that appear to define and differentiate specific chemical layers, even when those features are weak in intensity.

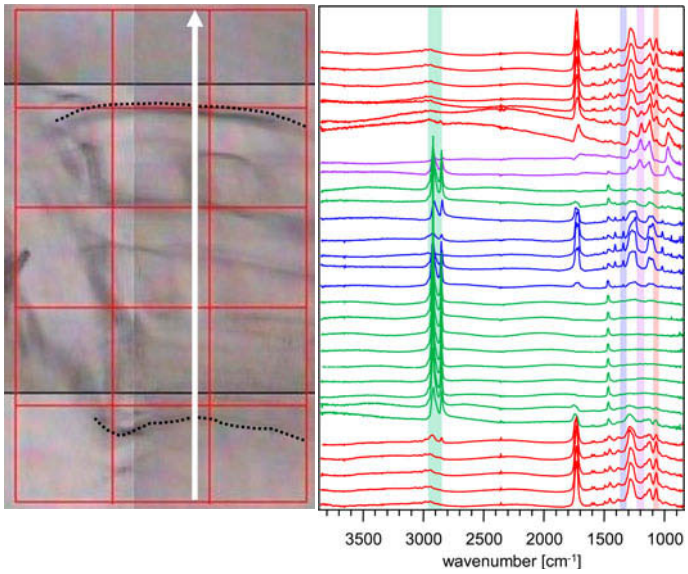

Figure 2: (A) Photomicrograph taken under white light illumination of the examined area of the layered oxygen barrier film; dashed lines indicate the top and bottom edges of the embedded cross-section. (B) Individual pixel SR-FTIR spectra extracted from along the path shown by the arrow in (A), showing the change in chemical signatures along the imaged area, from the bottom to the top of the sample. Each spectrum is an average of 32 scans. Colored bars identify spectral features that may be used to differentiate the four different organic materials present in the imaged area (see text).

Integration over selected characteristic peaks for each component (following baseline correction for each selected peak) produces chemical images for each component. Chemical images resulting from the integration of the characteristic peaks marked with colored bars in Figure 2b are shown in Figure 3. The top CTFE layer is identifiable by a C-F band centered at 1200 cm^{-1},[40] the polyethylene layers by the strong features in the CH-stretching region (centered at 2850 cm^{-1} and 2919 cm^{-1}), the internal polyester layer by a weak band at 1342 cm^{-1}, and the polyester embedding resin by a medium intensity feature at 1068 cm^{-1}. Other bands could as easily have been chosen to create images of each layer. Indeed, to confirm that a chemical species is related to a specific layer, it would be necessary to localize multiple bands from that species.

As shown in Figure 3, the layers present in the film can be quite effectively visualized using the chemical images. However, it must be noted that this was an ideal sample, containing spectroscopically distinct materials found in discrete layers, and prepared as a thin section for transmission analysis. While some samples found in cultural heritage research may share these characteristics, the vast majority of samples will not. Most "real-world" samples will have inhomogeneity within individual layers, have

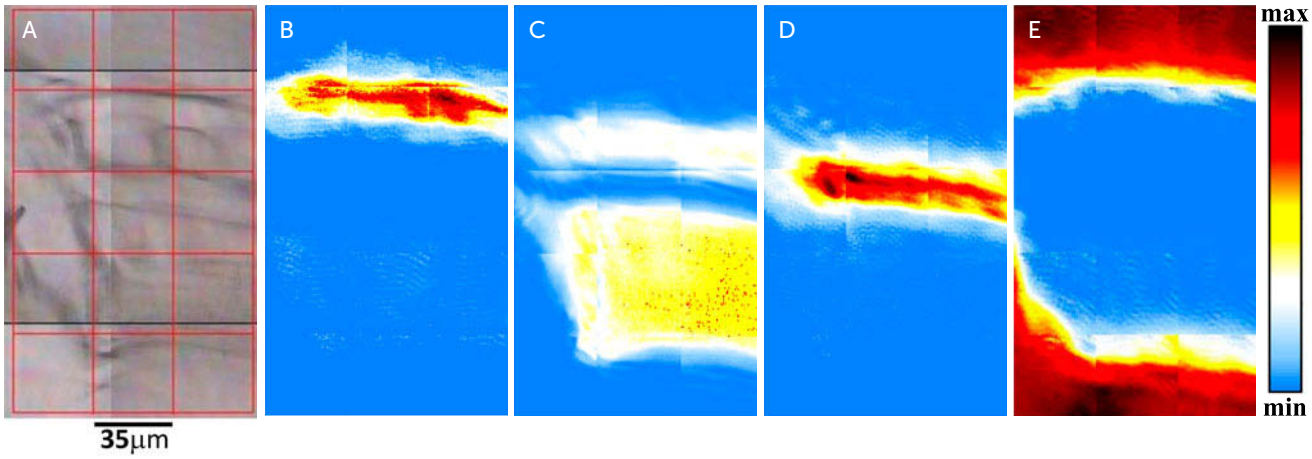

Figure 3: Photomicrograph of the examined area (A) and chemical images (B-E) of a portion of a mounted cross-section of FR-7750 film. Data taken in transmission, 32 scans averaged per pixel, >61,000 spectra in overall image, total acquisition time ~20 min. Chemical images show integration from (B) 1180-1221 cm^{-1}, (C) 2829-2866 cm^{-1}, (D) 1335-1352 cm^{-1}, and (E) 1053-1090 cm^{-1}. Color scales are different for each image.

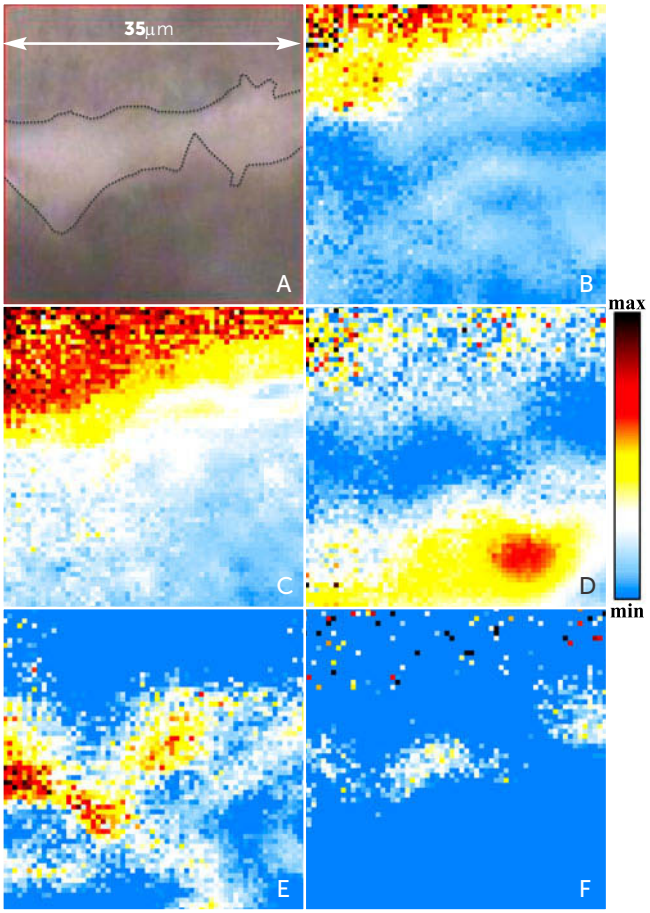

Figure 4: Photomicrograph of the examined area (A) and chemical images (B-E) of a portion of a mounted cross-section with multiple proteinaceous layers. Dashed lines in A indicate the boundaries between layers. Data taken in transmission, 128 scans averaged per pixel, 4,096 spectra in overall image, total acquisition time ~4.5 min. Chemical images show integration from (B) 1718-1761 cm^{-1}, (C) 2829-2995 cm^{-1}, (D) 1041-1215 cm^{-1}, (E) 1309-1358 cm^{-1}. Panel (F) shows the result of subtracting image (D) from (E). Color scales are different for each image.

rougher surfaces, and contain more complex mixtures of organic materials, inorganic materials, and, perhaps, their degradation products.

A more representative scenario for cultural heritage samples is presented by a sample, shown in Figure 4a, that contains a gypsum ground layer (likely with a glue binder), a layer of rabbit skin glue (simulating a sizing layer), and a layer of egg yolk (simulating an egg tempera paint layer). All three of these layers contains proteinaceous organic material and are therefore challenging to identify while retaining the spatial integrity of the sample. This sample is also more friable than the film sample discussed above, and substantially more absorbing of IR radiation, possibly due in part to increased scattering or rougher surface of the inhomogeneous material. The practical results of this are that prepared thin sections have fewer intact areas for analysis, and individual pixels imaged from within that area may be fully absorbing, resulting in pixels that contain no chemical information. Fortunately however, perhaps a benefit of the inhomogeneities in the sample, a majority of the pixels remain useful. The high signal-to-noise spectra produced by the synchrotron results in an overall image that contains spatially resolved chemical information, and areas containing all three layers could be identified for analysis.

The top layer containing egg yolk can be spatially located by the strong carbonyl (~1740 cm^{-1}, Figure 4b) and CH stretches (2842 cm^{-1}/2924 cm^{-1}, Figure 4c), both associated with the lipid components in egg yolk.[9] The bottom, gypsum ground, layer can be identified by the strong sulfate stretching band at ~1134 cm^{-1} (Figure 4d).[41] The rabbit skin glue layer is the most challenging layer to isolate, since it produces a spectrum containing little that is unique compared to the proteins found in the layers above and below it. A very weak feature near 1300 cm^{-1} appears to correlate with the bottom portion of the imaged area (Figure 4e), and may be related to the glue content present in both the rabbit skin glue and ground layers. Subtracting the image that localizes gypsum from the image that localizes the 1300 cm^{-1} band clearly separates the rabbit skin glue from the glue-gypsum layer (Figure 4f).

Because the layers can be isolated spectroscopically and spatially in this manner, spectra from either individual pixels, or averages of pixels from selected areas within a layer, may be extracted. If the identity of the layer were unknown, or if more information was desired for a specific layer, as is likely to be the case in a cultural heritage sample, the extracted spectra provides a high signal-to-noise spectrum for further analysis. The analysis of this more realistic sample, and the ability to mine the data for chemical information regarding even chemically similar layers, suggests that the IRENI beamline will be capable of identifying and spatially locating the components in complicated cultural heritage samples.

3.2 Application to Cultural Heritage Samples

Several samples from Matisse's *Le Bonheur de vivre* (BF719; Figure 5a) were analyzed using IRENI; partial results from one sample are presented here. The painting has recently been the focus of intensive analytical study as part of the development of a conservation plan and to elucidate yellow pigment degradation mechanisms.[42-44] A sample from a section of cadmium yellow (CdS) paint undergoing photodegradation (visible in the formation of an off-white crust at the top surface of the sample) from the region below the central reclining figures, was analyzed, and is shown in Figure 5b. Due to the non-rectangular shape of the sample, the left and right sides of the sample were measured separately to economize the time required to measure the full cross-section.

Previous work by Mass et al. by microRaman, microFTIR, X-ray absorption near-edge structure (XANES), and X-ray photoelectron spectroscopy (XPS) has indicated that cadmium carbonate is present in some areas of degraded pigment.[42-44] Since $CdCO_3$ can be present either as remaining starting material from the wet process manufacture of CdS or as evidence of a photodegradation pathway, and photo-induced degradation typically occurs in the top 1-5 μm of the paint layer (although thicker crusts have been observed for severe cases of photodegradation),[45] the distribution of the species is of interest to help clarify

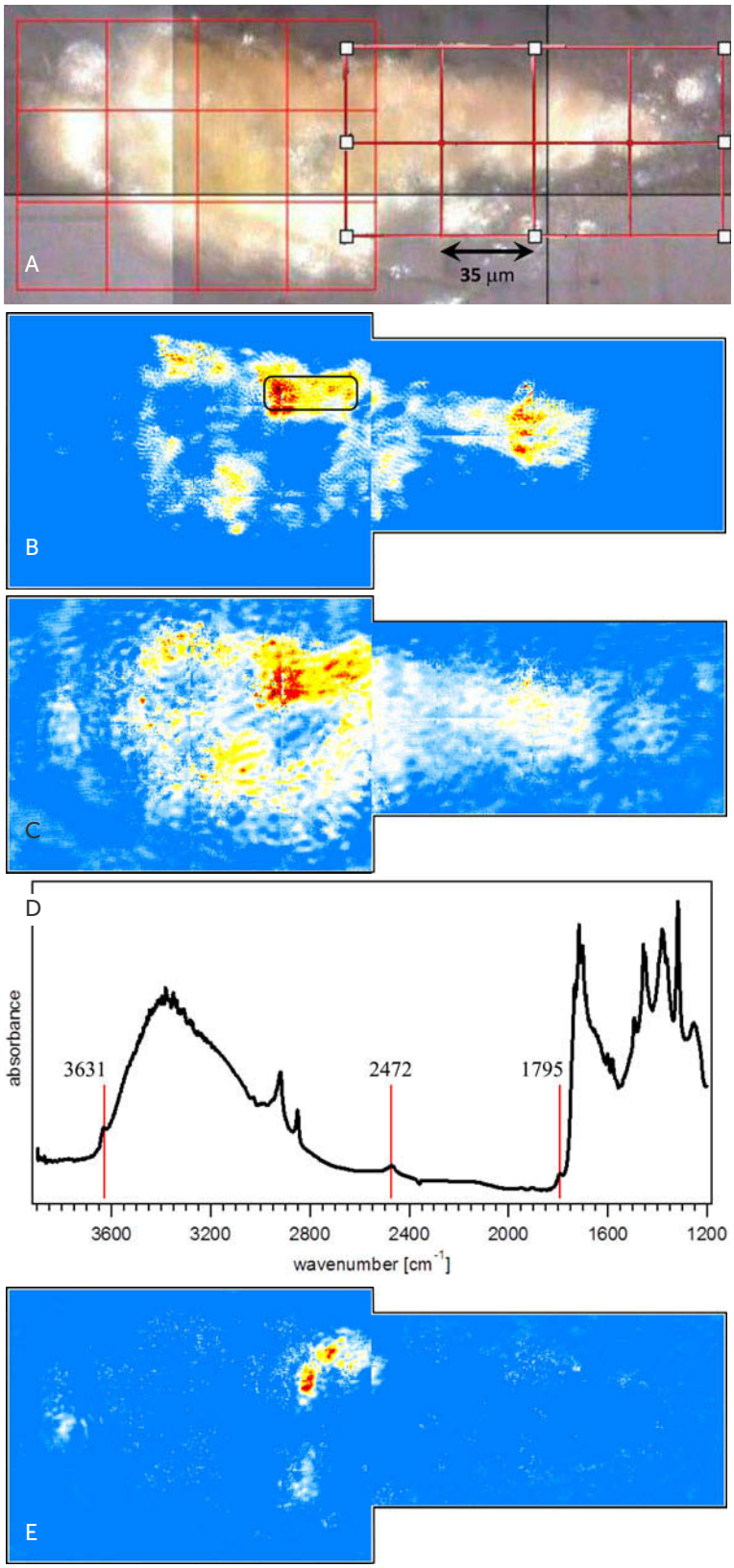

Figure 5: (A) photomicrographs of examined areas from Le Bonheur de vivre, also called The Joy of Life by Henri Matisse (oil on canvas, 176.5×240.7 cm (69 1/2×94 3/4 in.), BF719, The Barnes Foundation. Chemical images to visualize the distribution of CdCO3 were made using integration from (B) 1778-1803 cm-1 and (C) 2442-2503 cm-1. (D) Average spectrum from area noted on Figure 5b, and (E) integration from 3606-3664 cm-1. Data taken in transmission, 256 scans averaged per pixel, >81,000 spectra in overall image. Color scales are different for each image.

the source of cadmium carbonate in samples from this painting.

Due to the small size and porosity of the analyzed sample, and resulting impregnation of the sample by the polyester mounting resin, peaks in the spectrally congested region below the carbonyl band of the polyester – including the strong asymmetric carbonate stretch near 1427 cm^{-1} in $CdCO_3$[46] – cannot reliably be utilized for analysis. However, the high quality of the data allows two weak combination bands expected for $CdCO_3$, centered at 1795 cm^{-1} ($\nu_1+\nu_4$; symmetric stretch+in-plane bending) and 2472 cm^{-1} ($\nu_1+\nu_3$; symmetric stretch+asymmetric stretch),[46] to be used as indicators of this species. The average spectrum for all examined pixels (not shown) confirms that the 2472 cm^{-1} band is present and can be used for identification of cadmium carbonate. The 1795 cm^{-1} band is less evident, but may be present as a weak shoulder. Integration over the 1795 cm^{-1} and 2472 cm^{-1} bands results in the chemical images shown in Figure 5c and 5d, respectively. While some carbonate appears to be present at each edge of the sample, there appears to be a region of elevated concentration of this species towards the top center portion of the sample, in the area indicated by a box in Figure 5c.

Figure 5e shows an average spectrum from this small region of interest, averaging 1,554 individual pixel spectra. Again, the low wavenumber range of the spectrum is spectrally congested and highly absorbing, probably due to the presence of organic binding media in the area and impregnation by the polyester mounting resin. However above ~1750 cm^{-1} several notable features can be observed in addition to the expected bands for cadmium carbonate at 2472 cm^{-1} and 1795 cm^{-1}. The unexpectedly sharp peaks in the CH stretching region (~2830 – 2950 cm^{-1}), for example, may be an indicator of the presence of wax, which has been observed in other samples from this painting, and may be evidence of a prior conservation treatment. Interestingly, a sharp, but weak, feature is present centered at 3631 cm^{-1}; this band was not observed in a reference spectrum of cadmium carbonate.

Integration over this unusual band, shown in Figure 5f, suggests it is present in a localized portion of the cross-section, and is only associated with the cadmium carbonate at the top of the cross-section. This band may be associated with a localized degradation product or inclusion of unknown composition. Species expected to have features in this region of the spectrum are primarily hydroxides. The spectral position of the observed band is not an exact match with known phases of cadmium hydroxide, which have bands at 3607 (β-$Cd(OH)_2$), 3588 (γ-$Cd(OH)_2$), and 3531 cm^{-1} (γ-$Cd(OH)_2$).[47-49] Other brucite-type metal

hydroxides ($M(OH)_2$ where M=Mn, Co, Ni, Fe, Ca), however, are known to have sharp bands in the range 3624-3645 cm^{-1}.[48] Further exploration of the molecular source of this small feature – the smaller lobe of which is on the order of only 8×8 μm^2 – will inform the on-going analysis of degradation processes in this painting and others containing cadmium yellow. Importantly, the spectra acquired using the novel IRENI instrumental setup are sufficiently high quality to localize this small, but potentially important, feature, in a short space of time, and with relatively little specialized sample preparation.

4 Conclusions and Future Directions

The IRENI beamline is unique in the field of synchrotron-based FTIR imaging because it enables wide-field, high resolution infrared imaging with the high throughput and signal-to-noise produced by a bright, stable synchrotron beam. Preliminary evaluation of the IRENI mid-IR synchrotron beamline indicates that the system will be capable of spatially resolved identification of both organic and, in some cases, inorganic materials in painting cross-sections, even when the layers are chemically similar. Due to the brightness advantage of the synchrotron source, the system has increased sensitivity compared to thermal instrumentation in transmission. This increased sensitivity allows even weak features, such as the combination bands utilized in the analysis of $CdCO_3$, or the very weak band associated with glue layers in the painting mock-up sample, to be identified and used to create high resolution chemical images of cultural heritage samples. The ability to utilize these low-intensity bands is likely to increase the ability to differentiate between chemically similar species, in particular in instances where the most intense diagnostic bands may be shared. Notably, for transmission measurements analysis can be performed with high spatial resolution and spectral quality without contact with the sample, as would be required for ATR-FTIR imaging (perhaps a more broadly accessible technology), avoiding the problem of both sample contamination between measurements and incidental damage to the sample surface from the pressure required to maintain adequate contact between an ATR objective and the sample under study.

Beyond the increased sensitivity and spatial resolution of the IRENI beamline, use of the system provides further benefits to cultural heritage community. Use of this (or any other imaging FTIR beamline) effectively amortizes of cost of the FPA detector, (>$100,000 in addition to the FTIR microscope system), over a community of users, making FTIR imaging available to institutions that may not otherwise be able to afford an FPA detector. The relatively large area over which data can be acquired in a single exposure due to the novel 12-beam arrangement at IRENI allows imaging experiments to be time-efficient, a critical factor since beam time is necessarily limited when working at a synchrotron facility.

Disadvantages of the system include the fact that the analysis is performed at an outside facility, the costs associated with beam time (modest facility fees, currently $140 USD/12 hours beam time, and travel expenses), and the specialization of the system, which is currently optimized for transmission experiments. Although sample preparation using an ultramicrotome provides both a thin section and the more traditional block face sample that is compatible with other analyses typically performed on cross-section samples, the success of the sample preparation is highly dependent on the nature (i.e. homogeneity, porosity, etc.) of the individual sample. Particularly friable samples may not be able to be prepared using the techniques employed in this work. Alternate means of sample preparation for both transmission and reflection samples are therefore being explored.[50,51]

In order to be more broadly applicable to the cultural heritage community, additional instrumental schemes – such as standard reflectance measurements and ATR modalities – are also currently being developed for IRENI. Having a variety of sample preparation methodologies and instrumental schemes available will enhance the possibilities of acquiring high spatial resolution molecular spectroscopy at IRENI. While synchrotron-based FTIR imaging spectroscopy will not be appropriate for every question raised by the analysis of works of art, the IRENI beamline does provide new capabilities ideally suited to address some of the challenges related to the analysis of small multi-layered samples.

5 Acknowledgements

This work was supported by the Getty Conservation Institute. The development of the IRENI beamline was supported by the US National Science Foundation under awards CHE-0832298, CHE-1112433, CHE-0957849, and MRI-DMR-0619759. The Synchrotron Radiation Center, University of Wisconsin-Madison is supported by the University of Wisconsin-Madison and the University of Wisconsin-Milwaukee. The authors also wish to thank Michael Nasse and Miriam Unger (formerly and currently at SRC, respectively) for help during data acquisition and analysis, and The Barnes Foundation and Barbara Buckley for gracious permission to publish ongoing work on the Matisse project.

6 References

1. W. C. McCrone, *The Microscopical Identification of Artists' Pigments,* J. Int. Inst. Conserv., 1982, **7**, 11-34.

2. D. Pinna, M. Galeotti, R. Mazzeo, Eds., *Scientific Examination for the Investigation of Paintings. A Handbook for Conservator-restorers*; Centro Di della Edifimi srl, Florence, 2009.

3. J. Wouters, *High Performance Liquid Chromatography of Anthraquinones: Analysis of Plant and Insect Extracts and Dyed Textiles,* Stud. Conserv., 1985, **30**, 119-128.

4. J. Wouters, A. Verhecken, *The Coccid Insect Dyes: HPLC and Computerized Diode-Array Analysis of Dyed Yarns,* Stud. Conserv., 1989, **34**, 189-200.

5. J. S. Mills, R. White, *The Organic Chemistry of Museum Objects,* 2nd ed., Butterworth-Heinemann, Oxford, 1994.

6. M. P. Colombini, F. Modugno, Eds., *Organic Mass Spectrometry in Art and Archaeology*; John Wiley & Sons, West Sussex, 2009.

7. J. Wouters, C. M. Grzywacz, A. Claro, *Markers for Identification of Faded Safflower Carthamus tinctorius L.) Colorants by HPLC-PDA-MS. Ancient Fibres, Pigments, Paints and Cosmetics Derived from Antique Recipes,* Stud. Conserv., 2010, **55**, 186-203.

8. J. Wouters, C. M. Grzywacz, A. Claro, *A Comparative Investigation of Hydrolysis Methods to Analyze Natural Organic Dyes by HPLC-PDA. Nine Methods, Twelve Biological Sources, Ten Dye Classes, Dyed Yarns, Pigments and Paints,* Stud. Conserv., 2011, **56**, 231-249.

9. M. R. Derrick, J. M. Landry, D. C. Stulik, *Methods in scientific examination of works of art : infrared microspectroscopy,* Getty Conservation Institute, Los Angeles, 1991.

10. F. Casadio, L. Toniolo, *The analysis of polychrome works of art: 40 years of infrared spectroscopic investigations,* J. Cult. Herit., 2001, **2**, 71-78.

11. K. Castro, M. Perez, M. D. Rodriguez-Laso, J. M. Madariaga, *FTIR Spectra Database of Inorganic Art Materials,* Anal. Chem., 2003, **75**, 214A-221A.

12. G. Bitossi, R. Giorgi, M. Mauro, B. Salvadori, L. Dei, *Spectroscopic techniques in cultural heritage conservation: A survey,* Appl. Spectrosc. Rev., 2005, **40**, 187-228.

13. K. Janssens, R. V. Grieken, Eds., *Non-destructive Micro Analysis of Cultural Heritage Materials*; Elsevier, New York, 2005.

14. E. L. Kendix, S. Prati, R. Mazzeo, E. Joseph, G. Sciutto, C. Fagnano, *Far Infrared Spectroscopy in the Field of Cultural Heritage,* e-Preserv. Sci., 2010, **7**, 8-13.

15. S. Prati, E. Joseph, G. Sciutto, R. Mazzeo, *New Advances in the Application of FTIR Microscopy and Spectroscopy for the Characterization of Artistic Materials,* Acc. Chem. Res., 2010, **43**, 792-801.

16. W. Vetter, M. Schreiner, *Characterization of Pigment-Binding Media Systems - Comparison of Non-Invasive In-Situ Reflection FTIR with Transmission FTIR Microscopy,* e-Preserv. Sci., 2011, **8**, 10-22.

17. E. Joseph, S. Prati, G. Sciutto, M. Ioele, P. Santopadre, R. Mazzeo, *Performance evaluation of mapping and linear imaging FTIR microspectroscopy for the characterisation of paint cross sections,* Anal. Bioanal. Chem., 2010, **396**, 899-910.

18. R. Sloggett, C. Kyi, N. Tse, M. J. Tobin, L. Puskar, S. P. Best, *Microanalysis of artworks: IR microspectroscopy of paint cross-sections,* Vibr. Spectrosc., 2010, **53**, 77-82.

19. J. Van der Weerd, H. Brammer, J. J. Boon, R. M. A. Heeren, *Fourier Transform Infrared Microscopic Imaging of an Embedded Paint Cross-Section,* Appl. Spectrosc., 2002, **56**, 275-283.

20. C. Ricci, S. Bloxham, S. G. Kazarian, *ATR-FTIR imaging of albumen photographic prints,* J. Cult. Herit., 2007, **8**, 387-395.

21. M. Cotte, E. Checroun, J. Susini, P. Walter, *Micro-analytical study of interactions between oil and lead compounds in paintings,* Appl. Phys. A, 2007, **89**, 841-848.

22. M. Spring, C. Ricci, D. A. Peggie, S. G. Kazarian, *ATR-FTIR imaging for the analysis of organic materials in paint cross sections: case studies on paint samples from the National Gallery, London,* Anal. Bioanal. Chem., 2008, **392**, 37-45.

23. J.-P. Echard, M. Cotte, E. Dooryhee, L. Bertrand, *Insights into the varnishes of historical musical instruments using synchrotron micro-analytical methods,* Appl. Phys. A, 2008, **92**, 77-81.

24. E. Joseph, C. Ricci, S. G. Kazarian, R. Mazzeo, S. Prati, M. Ioele, *Macro-ATR-FT-IR spectroscopic imaging analysis of paint cross-sections,* Vib. Spectrosc., 2010, **53**, 274-278.

25. M. J. Nasse, B. Bellehumeur, S. Ratti, C. Olivieri, D. Buschke, J. Squirrell, K. Eliceiri, B. Ogle, C. S. Patterson, M. Giordano, C. J. Hirschmugl, *Opportunities for multiple-beam synchrotron-based mid-infrared imaging at IRENI,* Vibr. Spectrosc., 2012, **60**, 10-15.

26. G. D. Smith, *Infrared Microspectroscopy Using a Synchrotron Source for Arts-Science Research,* J. Am. Inst. Conserv., 2003, **42**, 399-406.

27. N. Salvadó, S. Buti, M. J. Tobin, E. Pantos, A. Prag, T. Pradell, *Advantages of the use of SR-FT-IR microspectroscopy: Applications to cultural heritage,* Anal. Chem., 2005, **77**, 3444-3451.

28. N. Salvadó, S. Butí, E. Pantos, F. Bahrami, A. Labrador, T. Pradell, *The use of combined synchrotron radiation micro FT-IR and XRD for the characterization of Romanesque wall paintings,* Appl. Phys. A, 2007, **90**, 67-73.

29. M. Cotte, P. Dumas, Y. Taniguchi, E. Checroun, P. Walter, J. Susini, *Recent applications and current trends in Cultural Heritage Science using synchrotron-based Fourier transform infrared micro-spectroscopy,* Physics and Heritage (Physique et patrimoine), 2009, **10**, 590-600.

30. M. Cotte, E. Checroun, V. Mazel, V. A. Solé, P. Richardin, Y. Taniguchi, P. Walter, J. Susini, *Combination of FTIR and X-rays Synchrotron-based Micro-Imaging Techniques for the Study of Ancient Paintings. A Practical Point of View,* e-Preserv. Sci., 2009, **6**, 1-9.

31. D. Creagh, A. Lee, V. Otieno-Alego, M. Kubik, *Recent and future developments in the use of radiation for the study of objects of cultural heritage significance,* Radiat. Phys. Chem., 2009, **78**, 367-374.

32. J.-P. Echard, L. Bertrand, A. von Bohlen, A.-S. Le Hô, C. Paris, L. Bellot-Gurlet, B. Soulier, A. Lattuati-Derieux, S. Thao, L. Robinet, B. Lavédrine, S. Vaiedelich, *The Nature of the Extraordinary Finish of Stradivari's Instruments,* Angew. Chem. Int. Ed., 2010, **49**, 197-201.

33. A. Lluveras, S. Boularand, A. Andreotti, M. Vendrell-Saz, *Degradation of azurite in mural paintings: distribution of copper carbonate, chlorides and oxalates by SRFTIR,* Appl. Phys. A, 2010, **99**, 363-375.

34. L. Bertrand, L. Robinet, M. Thoury, K. Janssens, S. X. Cohen, S. Schöder, *Cultural heritage and archaeology materials studied by synchrotron spectroscopy and imaging,* Appl. Phys. A, 2012, **106**, 377-396.

35. L. Bertrand, M. Cotte, M. Stampanoni, M. Thoury, F. Marone, S. Schöder, *Development and trends in synchrotron studies of ancient and historical materials,* Phys. Rep., 2012, **519**, Pages 51-96.

36. M. J. Nasse, M. J. Walsh, E. C. Mattson, R. Reininger, A. Kajdacsy-Balla, V. Macias, R. Bhargava, C. J. Hirschmugl, *High-resolution Fourier-transform infrared chemical imaging with multiple synchrotron beams,* Nat. Meth., 2011, **8**, 413-416.

37. M. J. Nasse, E. C. Mattson, R. Reininger, T. Kubala, S. Janowski, Z. El-Bayyari, C. J. Hirschmugl, *Multi-beam synchrotron infrared chemical imaging with high spatial resolution: Beamline realization and first reports on image restoration,* Nucl. Instr. Meth. Phys. Res. Sect. A, 2011, **649**, 172-176.

38. M. J. Nasse, http://www.iridys.com/ (accessed 14/01/2013).

39. M. Shin, K. Elert, *The Use of Oxygen-Free Environments in the Control of Museum Insect Pests*, The Getty Conservation Institute, Los Angeles, 2003.

40. D. J. T. Hill, K. J. Thurecht, A. K. Whittaker, *New Structure Formation on -irradiation of Polychlorotrifluoroethylene,* Radiat. Phys. Chem., 2003, **67**, 729-736.

41. H. Böke, S. Akkurt, S. Özdemir, E. H. Göktürk, E. N. Caner Saltik, *Quantification of CaCO3–CaSO3·0.5H2O–CaSO4·2H2O mixtures by FTIR analysis and its ANN model,* Mater. Lett., 2004, **58**, 723-726.

42. J. Mass, B. Buckley, M. Little, *The Photo-Oxidative Degradation of Matisse's Le Bonheur de Vivre (1905-6): X-Ray Based Methods for Degradation Mechanism Identification*, in 59th Annual Denver X-Ray Conference, Denver, CO, 2010.

43. J. Mass, *The Materials Chemistry of Paintings: Uncovering Hidden Images and Diagnosing Fading Masterpieces*, in 241st American Chemical Society National Meeting, Anaheim, CA, 2011.

44. J. Mass, J. Church, F. Fang, R. Opila, I. Shah, A. Mehta, J. Moulder, M. Cotte, B. Buckley, *Synchrotron Studies of Pigment Degradation*, in Synchrotron Research in Cultural Heritage Science Symposium, Chicago, IL, 2011.

45. F. Casadio, S. Xie, S. C. Rukes, B. Myers, K. A. Gray, R. Warta, I. Fiedler, *Electron energy loss spectroscopy elucidates the elusive darkening of zinc potassium chromate in Georges Seurat's A Sunday on La Grande Jatte—1884,* Anal. Bioanal. Chem., 2011, **399**, 2909-2920.

46. M. E. Bottcher, P.-L. Gehlken, *FT-IR Spectroscopic Characterization of (Ca, Cd)CO3 Solid Solutions: Compositional and Carbon Isotope Effects,* Appl. Spectrosc., 1997, **51**, 130-131.

47. M. Schmidt, H. D. Lutz, *y-Cd(OH)2, A common hydroxide or an aquoxy-hydroxide?,* Mat. Res. Bull., 1991, **26**, 605-612.

48. B. Weckler, H. D. Lutz *Near-infrared spectra of M(OH)C1 (M = Ca, Cd, Sr), Zn(OH)F, 7-Cd(OH)2, Sr(OH)2, and brucite-type hydroxides M(OH)2 (M- Mg, Ca, Mn, Fe, Co, Ni, Cd),* Spectrochim. Acta A, 1996, **52**, 1507-1513.

49. M. Ristić, S. Popović, S. Musić, *Formation and properties of Cd(OH)2 and CdO particles,* Mater. Lett., 2004, **58**, 2494-2499.

50. J. v. d. Weerd, R. M. A. Heeren, J. J. Boon, *Preparation Methods and Accessories for the Infrared Spectroscopic Analysis of Multi-LayerPaint Films,* Stud. Conserv., 2004, **49**, 193-210.

51. R. Mazzeo, E. Joseph, S. Prati, A. Millemaggi, *Attenuated Total Reflection–Fourier transform infrared microspectroscopic mapping for the characterisation of paint cross-sections,* Anal. Chim. Acta, 2007, **599**, 107-117.